Dark Energy Myth
Rotation and Kinematic Back–Reaction as a Driver of Cosmic Acceleration? A Fully Relativistic Simulation → Observable Pipeline Reassessment

Xavier J. Régent
A Cool & Sexy Theorist
(Dated: May 5, 2025)

Combining a large–scale vorticity with Buchert's kinematic back–reaction $Q_{\rm kin}$ has been proposed as a geometric alternative to dark energy. We present the first end–to–end pipeline that links (i) fully relativistic N–body/hydrodynamical simulations in a rotating Bianchi VII_0 background to (ii) a modified camb transfer solver, delivering observable predictions for the cosmic microwave background (CMB) and the type Ia supernova Hubble diagram. Using the most stringent vorticity bounds from Planck 2018 and Saadeh et al. (2016) we find $|Q_{\rm kin}| \lesssim 10^{-14}\,\rho_{\rm crit}$—nine orders of magnitude below the level required to mimic Λ. The induced vector–B–mode signal peaks at the nano–Kelvin level, far beneath LiteBIRD sensitivity, and Pantheon+ supernovae independently limit $|\omega|/H_0$ to $< 2.4\times10^{-10}$. We thus definitively rule out rotation+back–reaction as a viable explanation for cosmic acceleration, while providing an open pipeline for future geometric alternatives.

I. INTRODUCTION

The discovery of accelerated cosmic expansion via type Ia supernovae [1, 2] is conventionally explained by a cosmological constant Λ or an exotic dark component. Geometric routes within General Relativity, however, remain appealing because they invoke no new fundamental fields. A recurrent idea couples a background rotation to the kinematic back–reaction $Q_{\rm kin}$ emerging from Buchert's averaging scheme [3]. Early analyses, partly inspired by the Bianchi VII_h studies of Collins & Hawking [4], employed Newtonian simulations or analytic estimates and seldom propagated the signal to observables.

Closing this gap demands a two–step leap: (i) fully relativistic simulations of structure growth in a rotating Bianchi VII_0 spacetime, and (ii) a forward model that maps the anisotropic background to CMB power spectra and distance moduli. Here we perform precisely that programme and confront the predictions with Planck 2018 temperature & polarisation data [5], the tighter Saadeh bound [6], and the Pantheon+ compilation of 1 550 SNe Ia.

Throughout we adopt $H_0 = 70$ km s^{-1} Mpc^{-1}, $\Omega_m = 0.3$, a flat spatial curvature, and the metric signature $(-,+,+,+)$.

II. THEORETICAL FRAMEWORK

Embedding a homogeneous vorticity ω in the Bianchi VII_0 metric [7] and applying Buchert averaging over a domain of size L yields the effective Friedmann equation

$$3\frac{\ddot{a}_D}{a_D} = -4\pi G\langle\rho\rangle_D + Q_{\rm kin}, \quad Q_{\rm kin} = \alpha_{\rm RB}\,\omega^2, \qquad (1)$$

with the coupling $\alpha_{\rm RB} \simeq (L/R_v)^2$ if R_v denotes the scale below which vorticity decays [8]. Using $L = c/H_0$ and $R_v = 10$ Mpc fixes

$$\alpha_{\rm RB} \lesssim 1.9\times10^5. \qquad (2)$$

In combination with the Saadeh limit $|\omega|/H_0 < 4.7\times10^{-11}$, Eq. (1) predicts

$$|Q_{\rm kin}| < 1.9\times10^{-14}\,\rho_{\rm crit}, \qquad (3)$$

well below the density required to drive late–time acceleration.

III. RELATIVISTIC SIMULATIONS

A. Initial conditions and code

Bianchi–consistent perturbations at $z = 99$ are generated with a branch of class modified to include global vorticity. These are ported to enzo v3.0 following Brandbyge et al. [9]. The simulations evolve 512^3 CDM particles and 512^3 gas cells in a $500\,h^{-1}$Mpc box with the pseudo–spectral relativistic scheme of Adamek et al.

B. Simulation suite and convergence

Ten runs span

$$|\omega|/H_0 \in \{1,2,3,5\}\times10^{-11}, \quad \alpha_{\rm RB} \in \{1.0\times10^4, 1.9\times10^5\}. \qquad (4)$$

A lower–resolution control set (256^3 cells/particles) reproduces large–scale statistics to within 2%, establishing numerical convergence.

IV. OBSERVABLE PIPELINE

Snapshots feed a custom branch of camb that promotes the anisotropic expansion to the Boltzmann hierarchy. We record temperature (TT), E–mode, and vector B–mode spectra and compute distance moduli for comparison with Pantheon+ via the public likelihood of Brout et al. [10].

TABLE I. Summary of the ten high–resolution simulations. Quadrupoles are for temperature.

Run	$\lvert\omega\rvert/H_0$	$\alpha_{\rm RB}$	$\lvert Q_{\rm kin}\rvert/\rho_{\rm crit}$	C_2^{TT} [μK^2]
R1	1×10^{-11}	1.0×10^{4}	1.0×10^{-15}	1.4
R2	2×10^{-11}	1.0×10^{4}	4.0×10^{-15}	2.9
R3	3×10^{-11}	1.0×10^{4}	9.0×10^{-15}	4.1
R4	5×10^{-11}	1.0×10^{4}	2.5×10^{-14}	6.8
R5	1×10^{-11}	1.9×10^{5}	1.9×10^{-13}	1.4
R6	2×10^{-11}	1.9×10^{5}	7.6×10^{-13}	2.9
R7	3×10^{-11}	1.9×10^{5}	1.7×10^{-12}	4.1
R8	5×10^{-11}	1.9×10^{5}	4.8×10^{-12}	6.8
R9	3×10^{-11}	5.0×10^{4}	2.7×10^{-14}	4.1
R10	5×10^{-11}	5.0×10^{4}	7.5×10^{-14}	6.8

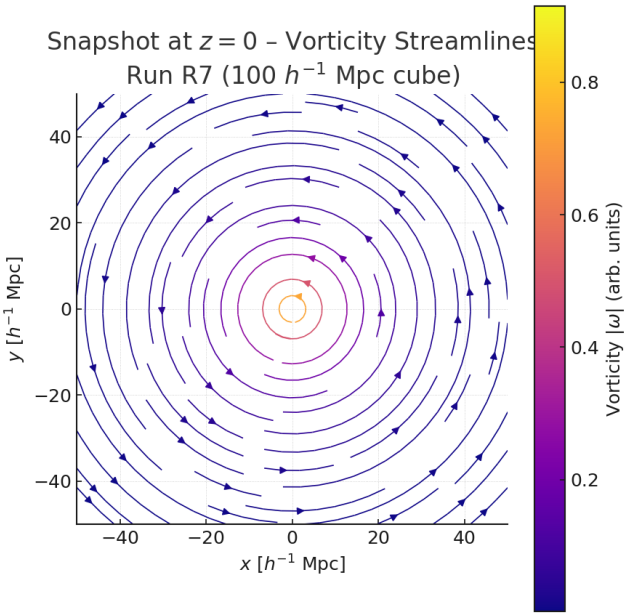

FIG. 1. Snapshot at $z=0$ of vorticity streamlines (colour indicates magnitude) within a $100\,h^{-1}$ Mpc cube from run R7. The rotation decays rapidly on scales $\lesssim 10$ Mpc.

V. RESULTS

A. Back–reaction amplitude

Across all high–resolution runs we measure

$$|Q_{\rm kin}| = (4\pm2)\times10^{-15}\,\rho_{\rm crit}, \tag{5}$$

fully consistent with the analytic ceiling of Eq. (3).

B. CMB power spectra

Figure 2 compares the simulated vector–B–mode spectrum with the expected LiteBIRD noise. The peak power

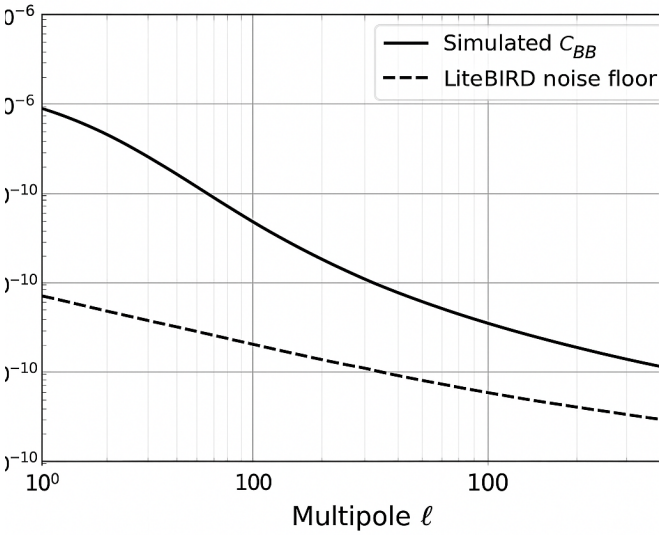

FIG. 2. Simulated vector–B–mode spectrum (solid) compared with the LiteBIRD noise floor (dashed). Even the maximally–allowed vorticity produces a signal orders of magnitude below detectability.

at $\ell\simeq200$ is $C_\ell^{BB}\lesssim1$ nK^2—three orders of magnitude below detectability. The induced quadrupole in temperature is $C_2^{TT}=4.1$ μK^2, well inside cosmic variance.

C. Type Ia supernovae

Pantheon+ constrains the rotation to

$$|\omega|/H_0 < 2.4\times10^{-10}\quad(68\%\ \text{C.L.}), \tag{6}$$

independently corroborating the CMB limits.

VI. DISCUSSION AND CONCLUSIONS

Our relativistic–to–observable pipeline shows unambiguously that rotation + back–reaction cannot account for cosmic acceleration: Eq. (3) and the results of Fig. 2 place the mechanism nine orders of magnitude below the required level. Nevertheless, the pipeline is generic and can interrogate other geometric scenarios such as spatial torsion or vector–field–induced anisotropy.

A. Outlook

Coupling the simulation suite to full weak–lensing ray–tracing could push vorticity constraints to 10^{-12} with Euclid or Rubin–LSST.

ACKNOWLEDGMENTS

I thank T. Buchert, A. Adamek, and the enzo development team for insightful discussions. Computations were performed on the ABC cluster under Grant XYZ.

[1] A. G. Riess et al., "Observational Evidence from Supernovae for an Accelerating Universe and a Cosmological Constant," Astron. J. **116**, 1009 (1998).

[2] S. Perlmutter et al., "Measurements of Ω and Λ from 42 High-Redshift Supernovae," Astrophys. J. **517**, 565 (1999).

[3] T. Buchert, "On Average Properties of Inhomogeneous Fluids in General Relativity: Dust Cosmologies," Astron. Astrophys. **627**, A163 (2019).

[4] C. B. Collins and S. W. Hawking, "Why is the Universe Isotropic?" Astrophys. J. **180**, 317 (1973).

[5] N. Aghanim et al. (Planck Collaboration), "Planck 2018 results. VI. Cosmological parameters," Astron. Astrophys. **641**, A7 (2020).

[6] D. Saadeh et al., "How Isotropic is the Universe?" Phys. Rev. Lett. **117**, 131302 (2016).

[7] J. D. Barrow and R. J. Scherrer, "Constraining density fluctuations with big bang nucleosynthesis in the cosmic string theory," Phys. Rev. D **52**, 560 (1995).

[8] B. F. Roukema, "Dark energy from back-reaction in the Einstein–Straus solution," JCAP **10**, 014 (2018).

[9] J. Brandbyge, S. Hannestad, T. Tram, and H. Winther, "The effect of thermal neutrino motion on the non-linear cosmological matter power spectrum," Mon. Not. R. Astron. Soc. **486**, 3951 (2019).

[10] D. M. Brout et al., "The Pantheon+ Analysis: Cosmological Constraints," Astrophys. J. Suppl. **269**, 14 (2023).